Interaction of CO_2 concentrations and water stress in semi-arid plants causes diverging response in instantaneous water use efficiency and carbon isotope composition

Na Zhao[1,3], Ping Meng[2], Yabing He[1], Xinxiao Yu[1,3]*

[1] College of soil and water conservation, Beijing Forestry University, Beijing 100083, P.R. China
[2] Research Institute of Forestry, Chinese Academy of Forestry 100091, Beijing, P.R. China
[3] Beijing collaborative innovation center for eco-environmental improvement with forestry and fruit trees

Abstract. In the context of global warming attributable to the increasing levels of CO_2, severe drought may be more frequent in areas with chronic water shortages (semi-arid areas). This necessitates research on the interactions between increased levels of CO_2 and drought on plant photosynthesis. It is commonly reported that ^{13}C fractionation occurred as CO_2-gas diffuses from the atmosphere to the sub-stomatal cavity. Few researchers have investigated ^{13}C fractionation at the site of carboxylation to cytoplasm before sugars are exported outward from the leaf. This process typically progresses in response to variations in environmental conditions (i.e., CO_2 concentrations and water stress), including in their interaction. Therefore, saplings of two typical plant species (*Platycladus orientalis* and *Quercus variabilis*) from semi-arid areas of Northern China were selected and cultivated in growth chambers with orthogonal treatments (four CO_2 concentrations ([CO_2]) × five soil volumetric water contents (SWC)). The $\delta^{13}C$ of water-soluble compounds extracted from leaves of saplings was determined for instantaneous water use efficiency (WUE_{cp}) after cultivation. Instantaneous water use efficiency derived from gas exchange (WUE_{ge}) was integrated to estimate differences in $\delta^{13}C$ signal variation before leaf-exported translocation of primary assimilates. The WUE_{ge} of *Platycladus orientalis* and *Quercus variabilis* both decreased with increased soil moisture at 35%–80% of field capacity (FC), and increased with elevated [CO_2] by increasing photosynthetic capacity and reducing transpiration. Instantaneous water use efficiency (iWUE) according to environmental changes, differed between the two species. The WUE_{ge} in *P. orientalis* was significantly greater than that in *Q. variabilis*, while an opposite trend was observed when comparing WUE_{cp} between the two species. Total ^{13}C fractionation at the site of carboxylation to cytoplasm before sugar export (total ^{13}C fractionation) was species-specific, as demonstrated in the interaction of [CO_2] and SWC. Rising [CO_2] coupled with moistened soil generated increasing disparities in $\delta^{13}C$ between water-soluble compounds ($\delta^{13}C_{WSC}$) and estimates based on gas-exchange observations ($\delta^{13}C_{obs}$) in *P. orientalis*, ranging between 0.0328‰–0.0472‰. Differences between $\delta^{13}C_{WSC}$ and $\delta^{13}C_{obs}$ in *Q. variabilis* increased as [CO_2] and SWC increased (0.0384‰–0.0466‰). The ^{13}C fractionation from mesophyll conductance (g_m) and post-carboxylation both contributed to the total ^{13}C fractionation that was determined by $\delta^{13}C$ of water-soluble compounds and gas-exchange measurement. Total ^{13}C fractionation was linearly dependent on stomatal conductance, indicating post-carboxylation fractionation could be attributed to environmental variation. The magnitude and environmental dependence of apparent post-carboxylation fractionation is worth our attention when addressing photosynthetic fractionation.

Key words: Post-carboxylation fractionation; Carbon isotope fractionation; Elevated CO_2 concentration; Soil volumetric water content; Instantaneous water use efficiency

1 Introduction

Since the industrial revolution, atmospheric CO_2 concentration has increased at an annual rate of 0.4%, and is expected to increase to 700 μmol·mol^{-1}, culminating in more frequent periods of dryness (IPCC, 2014). Increasing atmospheric CO_2 concentrations that exacerbate the greenhouse effect will increase fluctuations in global precipitation patterns, but will probably amplify drought frequency in arid regions, and lead to more frequent extreme events in humid regions (Lobell et al., 2014). Accompanying the increasing concentration of CO_2, mean $\delta^{13}C$ of atmospheric CO_2 is currently being depleted by 0.02‰–0.03‰ year^{-1} (CU-INSTAAR/NOAACMDL network for atmospheric CO_2; http://www.esrl.noaa.gov/gmd/).

The current carbon isotopic composition may respond to environmental change and their influence on diffusion via plant physiological and metabolic processes (Gessler et al., 2014; Streit et al., 2013). While depletion of $\delta^{13}C_{CO_2}$ is occurring in the atmosphere, variations in CO_2 concentration ($[CO_2]$) may affect $\delta^{13}C$ of plant organs that, in turn, are responding physiologically to changes in climate (Gessler et al., 2014). The carbon discrimination ($^{13}\Delta$) of leaves could also provide timely feedback about the availability of soil moisture and the atmospheric vapor pressure deficit (Cernusak et al., 2012). Discrimination of ^{13}C in leaves relies mainly on environmental factors that affect the ratio of intercellular to ambient $[CO_2]$ (C_i/C_a). Rubisco activities and the mesophyll conductance derived from the difference of $[CO_2]$s between intercellular sites and chloroplasts are also involved (Farquhar et al., 1982; Cano et al., 2014). Changes in environmental conditions affect photosynthetic discrimination and they will be recorded differentially in the $\delta^{13}C$ of water-soluble compounds ($\delta^{13}C_{WSC}$) in different plant organs. Several processes during photosynthesis alter the $\delta^{13}C$ of carbon transported within plants. Carbon-fractionation during photosynthetic CO_2 fixation has been reviewed elsewhere (Farquhar et al., 1982; Farquhar and Sharkey, 1982).

Post-photosynthetic fractionation is derived from equilibrium and kinetic isotopic effects that determine isotopic differences between metabolites and intramolecular reaction positions. These are defined as "post-photosynthetic" or "post-carboxylation" fractionation (Jäggi et al., 2002; Badeck et al., 2005; Gessler et al., 2008). Post-carboxylation fractionation in plants includes the carbon discrimination that follows carboxylation of ribulose-1, 5-bisphosphate, and internal diffusion (RuBP, 27‰), as well as related transitory starch metabolism (Gessler et al., 2008; Gessler et al., 2014) fractionation in leaves, fractionation-associated phloem transport, remobilization or storage of soluble carbohydrates, and starch metabolism fractionation in sink tissue (tree rings). In the synthesis of soluble sugars, ^{13}C-depletions of triose phosphates occur during exportation from the cytoplasm, and during production of fructose-1, as does 6-bisphosphate by aldolase in transitory starch synthesis (Rossmann et al., 1991; Gleixner and Schmidt, 1997). Synthesis of sugars before transportation to the twig is associated with the post-carboxylation fractionation generated in leaves. Although these are likely to play a role, another consideration is $[CO_2]$ in the chloroplast (C_c), not in the intercellular space, as used in the simplified equation of the Farquhar's model (Evans et al., 1986; Farquhar et al., 1989) is actually defined as carbon isotope discrimination ($\delta^{13}C$). Differences between gas-exchange derived values and online measurements of $\delta^{13}C$ have often been used to estimate C_i-C_c and mesophyll conductance for CO_2 (Le Roux et al., 2001; Warren and Adams, 2006; Flexas et al., 2006; Evans et al., 2009; Flexas et al., 2012; Evans and von Caemmerer 2013). In this regard, changes in mesophyll conductance could be partly responsible for the differences in two measurements, as it generally increases in the short term in response to elevated CO_2 (Flexas et al., 2014), but it tends to decrease under drought (Hommel et al., 2014; Théroux-Rancourt et al., 2014). Therefore, it is necessary to avoid confusion between carbon isotope discrimination derived from synthesis of soluble sugars and/or mesophyll conductance. The degree to magnitude of carbon fractionations is related to environmental variation has yet to be fully investigated.

The simultaneous isotopic analysis of leaves allows determination of temporal variation in isotopic fractionation (Rinne et al., 2016). This will aid the accurate recording of environmental conditions. Newly assimilated carbohydrates can be extracted, and these are termed the water-soluble compounds (WSCs) in leaves (Brandes et al., 2006; Gessler et al., 2009). WSCs can also be associated with an assimilation-weighted mean of C_i/C_a (and C_c/C_a) photosynthesized over periods ranging from a few hours to 1–2 d (Pons et al., 2009). However, there is disagreement whether fractionation caused by post-carboxylation and/or mesophyll resistance can alter the stable signatures of leaf carbon and thence influence instantaneous water use efficiency (iWUE). In addition, the manner in which iWUE derived from these isotopic fractionations responds to environmental factors, such as elevated [CO_2] and/or soil water gradients, is unknown.

Consequently, we investigated the $\delta^{13}C$ of fast-turnover carbohydrate pool in sapling leaves of two tree species, *Platycladus orientalis* (L.) Franco and *Quercus variabilis* Bl., native to semi-arid areas of China. We conducted gas-exchange measurements in controlled environment growth chambers (FH-230, Taiwan Hipoint Corporation, Kaohsiung City, Taiwan). One goal is to differentiate the ^{13}C fractionation from the site of carboxylation to cytoplasm prior to sugars transportation in *P. orientalis* and *Q. variabilis*, that is the total ^{13}C fractionation, determined from the $\delta^{13}C$ of WSCs and gas-exchange measurements. The other one is to discuss the potential causes for the observed divergence, estimate contributions of post-photosynthesis and mesophyll conductance on these differences, and describe how carbon isotopic fractionations respond to the interactive effects of elevated [CO_2] and water stress.

2 Material and Methods

2.1 Study site and design

P. orientalis and *Q. variabilis* saplings, selected as experimental material, were obtained from the Capital Circle forest ecosystem station, a part of Chinese Forest Ecosystem Research Network (CFERN), 40°03'45"N, 116°5'45"E in Beijing, China. This region is forested by *P. orientalis* and *Q. variabilis*. We chose saplings with similar basal diameters, heights, and growth classes. Each sapling was placed into an individual pot (22 cm diam. × 22 cm high). Undisturbed soil samples were collected from the field, sieved (with particles >10 mm removed), and placed into the pots. The soil bulk density in the pots was maintained at 1.337–1.447 g·cm^{-3}. After a 30 d transplant recovery period, the saplings were placed into growth chambers for orthogonal cultivation.

The controlled experiment studies were conducted in growth chambers (FH-230, Taiwan Hipoint Corporation, Kaohsiung City, Taiwan). To reproduce the meteorological factors of different growth seasons in the research region, daytime and nighttime temperatures in the chambers were set to 25 ± 0.5℃ from 07:00 to 17:00 and 18 ± 0.5℃ from 17:00 to 07:00. Relative humidity was maintained at 60% and 80% during the daytime and nighttime, respectively. The mean daytime light intensity was 200–240 μmol·m^{-2}·s^{-1}. The chamber control system can control and monitor [CO_2]. Two growth chambers (A and B) were used in this study. Chamber A maintained [CO_2]s at 400 ppm (C_{400}) and 500 ppm (C_{500}). Chamber B maintained [CO_2]s at 600 ppm (C_{600}) and 800 ppm (C_{600}). The target [CO_2] in the chambers had a standard deviation of ± 50 ppm during plant cultivation and testing.

An automatic watering device was used to irrigate the potted saplings and it can avoid heterogeneity when scheduled watering was not made (Fig. 1). The watering device consisted of a water storage tank, holder, controller, soil moisture sensors, and drip irrigation components. Prior to use, the tank was filled with water, and the soil moisture sensor was inserted to a uniform depth in the soil. After connecting the controller to an AC power supply, target soil volumetric water content (SWC) could be set and monitored by soil moisture sensors. Since timely SWC could be sensed by the sensors, this automatic watering device can be regulated to begin watering or stop watering the plants. One irrigation device was installed per chamber. Based on mean field capacity (FC) of potted soil (30.70%) combining [CO_2] gradient, we established the orthogonal treatments for four [CO_2]s × five SWCs (Tab. 1). In Table 1, A_1-A_4 denotes [CO_2] of 400 ppm (C_{400}), 500 ppm (C_{500}), 600 ppm (C_{600}) and 800 ppm (C_{800}) in the chambers. B_1-B_5 denotes 35%–45% of FC (10.74%–13.81%), 50%–60% of FC (15.35%–18.42%), 60%–70% of FC (18.42%–21.49%), and 70%–80% of FC (21.49%–24.56%) and 100% of FC (CK, 27.63%–30.70%). Each orthogonal treatment of [CO_2] × SWC for two saplings per species repeated twice. Each treatment lasted 7 d. One pot was exposed in one [CO_2] × SWC treatment. Pots in chambers were rearranged to promote uniform illumination every two days.

2.2 Foliar gas exchange measurement

Fully expanded primary annual leaves of the saplings were measured with a portable infrared gas photosynthesis system (LI-6400, Li-Cor, Lincoln, US) before and after the 7-day cultivation. Two saplings per specie were replicated per treatment (SWC× [CO_2]). For each sapling, four leaves were sampled and four measurements were conducted on each leaf. Main photosynthetic parameters, such as net photosynthetic rate (P_n) and transpiration rate (T_r), were measured. Based on the theories proposed by Von Caemmerer and Farquhar (1981), stomatal conductance (g_s) and intercellular [CO_2] (C_i) were calculated by the Li-Cor software. Instantaneous water use efficiency via gas exchange (WUE_{ge}) was calculated as the ratio P_n / T_r.

2.3 Plant material collection and leaf water-soluble compounds extraction

Eight recently-expanded sun leaves were selected per sapling and homogenized in liquid nitrogen after gas-exchange measurements were finished. For extraction of WSCs from the leaves (Gessler et al., 2004), 50 mg of ground leaves and 100 mg of PVPP (polyvinylpolypyrrolidone) were mixed and incubated in 1 mL distilled water for 60 min at 5℃ in a centrifuge tube. Each leaf was replicated twice. Two saplings per specie were chosen for each orthogonal treatment. The tubes containing the above mixture were heated in 100℃ water for 3 min. After cooling to room temperature, the supernatant of the mixture was centrifuged (12000 × *g* for 5 min) and 10 μL of supernatant was transferred into a tin capsule and dried at 70℃. Folded capsules were used for $\delta^{13}C$ analysis of WSCs. The samples of WSCs from leaves were combusted in an elemental analyzer (EuroEA, HEKAtech GmbH, Wegberg, Germany) and analyzed with a mass spectrometer (DELTA[plus]XP, ThermoFinnigan).

Carbon isotope signatures are expressed in δ-notation (parts per thousand), relative to the international Pee Dee Belemnite (PDB).

$$\delta^{13}C = \left(\frac{R_{sample}}{R_{standard}} - 1\right) \times 1000 \quad (1)$$

where $\delta^{13}C$ is the heavy isotope and R_{sample} and $R_{standard}$ refer to the isotope ratio between the particular substance and the corresponding standard, respectively. The precision of repeated measurements was 0.1 ‰.

2.4 Isotopic calculation

2.4.1 ^{13}C fractionation from the site of carboxylation to cytoplasm prior to sugars transportation

Based on the linear model developed by Farquhar and Sharkey (1982), the isotope discrimination, *Δ*, is calculated as

$$\Delta = (\delta^{13}C_a - \delta^{13}C_{WSC})/(1 + \delta^{13}C_{WSC}), \tag{2}$$

where $\delta^{13}C_a$ and $\delta^{13}C_{WSC}$ are the isotope signatures of ambient [CO_2] in chambers and WSCs extracted from leaves, respectively. The C_i:C_a is determined by

$$C_i : C_a = (\Delta - a)/(b - a), \tag{3}$$

where C_i and C_a are the [CO_2]s within substomatal cavities and in the growth chambers, respectively; a is the fractionation occurring CO_2 diffusion in still air (4‰) and b refers to the discrimination during CO_2 fixation by ribulose 1,5- bisphosphate carboxylase/oxygenase (Rubisco) and internal diffusion (30‰). Instantaneous water use efficiency by gas-exchange measurements (WUE$_{ge}$) is calculated as

$$\mathrm{WUE_{ge}} = P_n : T_r = (C_a - C_i)/1.6\Delta e, \tag{4}$$

where 1.6 is the diffusion ratio of stomatal conductance for water vapor to CO_2 in chambers and Δe is the difference between e_{lf} and e_{atm} that represent the extra- and intra-cellular water vapor pressure, respectively:

$$\Delta e = e_{lf} - e_{atm} = 0.611 \times e^{17.502\mathrm{T}/(240.97+\mathrm{T})} \times (1 - \mathrm{RH}), \tag{5}$$

where *T* and RH are the temperature and relative humidity on leaf surface, respectively. Combining Eqns. (2, 3 and 4), the instantaneous water use efficiency could be determined by the $\delta^{13}C_{WSC}$ of leaves, defined as:

$$\mathrm{WUE_{cp}} = \frac{P_n}{T_r} = (1-\varphi)(C_a - C_i)/1.6\Delta e = C_a(1-\varphi)\left[\frac{b - \delta^{13}C_a + (b+1)\delta^{13}C_{WSC}}{(b-a)(1+\delta^{13}C_{WSC})}\right]/1.6\Delta e, \tag{6}$$

where φ is the respiratory ratio of leaf carbohydrates to other organs at night (0.3).

Then the ^{13}C fractionation from the site of carboxylation to cytoplasm prior to sugars transportation (defined as the total ^{13}C fractionation) can be estimated by the observed δ^{13}C of WSCs from leaves ($\delta^{13}C_{WSC}$) and the modeled δ^{13}C calculated from gas-exchange measurements ($\delta^{13}C_{model}$). The $\delta^{13}C_{model}$ is calculated from Δ_{model} from Eqn. (2). The Δ_{model} can be determined by Eqns. (3 and 4) as

$$\Delta_{model} = (b-a)\left(1 - \frac{1.6\Delta e \mathrm{WUE_{ge}}}{C_a}\right) + a, \tag{7}$$

$$\delta^{13}C_{model} = \frac{C_a - \Delta_{model}}{1 + \Delta_{model}}, \tag{8}$$

$$\text{Total } ^{13}\text{C fractionation} = \delta^{13}C_{WSC} - \delta^{13}C_{model}. \tag{9}$$

2.4.2 Method of estimations for mesophyll conductance and the contribution of post-carboxylation fractionation

The carbon isotope discrimination is generated from the relative contribution of diffusion and carboxylation, reflected by the ratio of [CO_2] at the site of carboxylation (C_c) to that in the ambient environment surrounding plants (C_a). The carbon isotopic discrimination (Δ) can be presented as (Farquhar et al. 1982):

$$\Delta = a_b \frac{C_a - C_s}{C_a} + a \frac{C_s - C_i}{C_a} + (e_s + a_l) \frac{C_i - C_c}{C_a} + b \frac{C_c}{C_a} - \frac{\frac{eR_D}{k} + f\Gamma_*}{C_a}, \tag{10}$$

where C_a, C_s, C_i, and C_c are the $[CO_2]$s in the ambient environment, at the boundary layer of the leaf, in the substomatal cavities, and at the sites of carboxylation, respectively; a_b is the CO_2 diffusional fractionation at the boundary layer (2.9‰); e_s is the discrimination for CO_2 diffusion when CO_2 enters in solution (1.1‰, at 25℃); a_l is the CO_2 diffusional fractionation in the liquid phase (0.7‰); e and f are carbon discriminations derived in dark respiration (R_D) and photorespiration, respectively; k is the carboxylation efficiency, and Γ^* is the CO_2 compensation point in the absence of dark respiration (Brooks and Farquhar,1985).

When gas in the cuvette is well stirred during gas-exchange measurements, diffusion occurring boundary layer could be neglected and Equation 10 can be shown as

$$\Delta = a \frac{C_a - C_i}{C_a} + (e_s + a_l) \frac{C_i - C_c}{C_a} + b \frac{C_c}{C_a} - \frac{\frac{eR_D}{k} + f\Gamma_*}{C_a}. \tag{11}$$

There is no consensus about the value of e, although recent measurements estimate it as ranging from 0-4‰. The value of f has been estimated to range from 8-12‰ (Gillon and Griffiths, 1997; Igamberdiev et al., 2004; Lanigan et al., 2008). As the most direct factor, the value of b which influence the calculation of g_m, which is thought to be approximately 30‰ in higher plants (Guy et al., 1993).

The difference of $[CO_2]$ between substomatal cavities and chloroplasts is omitted while diffusions related to dark-respiration and photorespiration are negligible and Equation 11 could be simplified as

$$\Delta_i = a + (b - a) \frac{C_i}{C_a}. \tag{12}$$

Equation 12 denotes the linear relationship between carbon discrimination and C_i/C_a. That underlines subsequent comparison between expected Δ (originating from gas-exchange, Δ_i, and actually measured Δ_{obs}), could evaluate the differences of $[CO_2]$ between intercellular air and sites of carboxylation that are the ^{13}C fractionation from mesophyll conductance. Consequently, g_m is calculated by subtracting the Δ_{obs} of Equation 11 from Δ_i (Equation 12):

$$\Delta_i - \Delta_{obs} = (b - e_s - a_l) \frac{C_i - C_c}{C_a} + \frac{\frac{eR_D}{k} + f\Gamma^*}{C_a} \tag{13}$$

and the P_n from Fick's first law is presented by

$$P_n = g_m (C_i - C_c). \tag{14}$$

Substituting Equation 14 into Equation 13 we obtain

$$\Delta_i - \Delta_{obs} = (b - e_s - a_l) \frac{P_n}{g_m C_a} + \frac{\frac{eR_D}{k} + f\Gamma^*}{C_a}, \tag{15}$$

$$g_m = \frac{(b - e_s - a_l) \frac{P_n}{C_a}}{(\Delta_i - \Delta_{obs}) - \frac{eR_D/k + f\Gamma^*}{C_a}}. \tag{16}$$

In calculation of g_m, terms of respiratory and photorespiratory could be ignored and e and f are assumed to be zero or to be cancelled out in the calculation of g_m.

Then Equation 16 can be transformed into

$$g_m = \frac{(b - e_s - a_l)\frac{P_n}{C_a}}{\Delta_i - \Delta_{obs}}. \quad (17)$$

Therefore, the contribution of post- carboxylation fractionation can be estimated by

$$Contribution\ of\ post - \text{carboxylation}\ fractionation = \frac{(\text{Total }^{13}\text{C fractionation} - \text{fractionation from mesophll conductance})}{\text{Total }^{13}\text{C fractionation}} \times 100\%. \quad (18)$$

3 Results

3.1 Foliar gas exchange measurements

When SWC increased between the treatments, P_n, g_s and T_r in *P. orientalis* and *Q. variabilis* peaked at 70%–80% of FC and/or 100% of FC (Fig. 2). The C_i in *P. orientalis* rose as SWC increased. It peaked at 60%–70% of FC and declined thereafter with increased SWC in *Q. variabilis*. The carbon uptake and C_i were significantly improved by elevated [CO_2] at all SWCs for the two species ($p < 0.5$). Greater increases of P_n in *P. orientalis* were found at 50%–70% of FC from C_{400} to C_{800}, which was at 35%–45% of FC in *Q. variabilis*. As water stress was reduced (at 70%–80% of FC and 100% of FC), reduction of g_s in *P. orientalis* was more pronounced with elevated [CO_2] at a given SWC ($p < 0.01$). Nevertheless, g_s of *Q. variabilis* in C_{400}, C_{500}, and C_{600} was significantly higher than in C_{800} at 50%–80% of FC ($p < 0.01$). Coordinated with g_s, T_r of the two species in C_{400} and C_{500} was significantly higher than in C_{600} and C_{800} except at 35%–60% of FC ($p < 0.01$, Figs. 2g and 2h). P_n, g_s, C_i and T_r of *Q. variabilis* was significantly greater than the corresponding values of *P. orientalis* ($p < 0.01$, Fig. 2).

3.2 δ^{13}C of water-soluble compounds in leaves

After observations of photosynthetic traits in leaves of the two species, the same leaves were immediately frozen and WSCs were extracted for all orthogonal treatments. The carbon isotope composition of WSCs ($\delta^{13}C_{WSC}$) of both species increased as SWC increased (Figs. 3a and 3b, $p < 0.01$). The mean $\delta^{13}C_{WSC}$ of *P. orientalis* and *Q. variabilis* ranged from -27.44 ± 0.155‰ to -26.71 ± 0.133‰, and from -27.96 ± 0.129‰ to -26.49 ± 0.236‰, respectively. The photosynthetic capacity varied with increased SWC and the mean $\delta^{13}C_{WSC}$ of the two species reached maxima at 70%–80% of FC. With gradual enrichment of [CO_2], mean $\delta^{13}C_{WSC}$ in both species declined when [CO_2] exceeded 600 ppm ($p < 0.01$). Except for C_{400} at 50%–100% of FC, the $\delta^{13}C_{WSC}$ of *P. orientalis* was significantly larger than that of *Q. variabilis* at any [CO_2] × SWC treatment ($p < 0.01$, Fig. 3).

3.3 Estimations of WUE_{ge} and WUE_{cp}

Figure 4a shows that increments of WUE_{ge} in *P. orientalis* under severe drought (i.e., 35%–45% of FC) were highest at any [CO_2], ranging from 90.70% to 564.65%. The WUE_{ge} in *P. orientalis* decreased as SWC increased, while values increased as [CO_2] increased. Differing from variation in WUE_{ge} of *P. orientalis* with moistened soil, WUE_{ge} in *Q. variabilis* increased slightly at 100% of FC in C_{600} or C_{800} (Fig. 4b). The maximum WUE_{ge} occurred at 35%–45% of FC in C_{800} among all orthogonal treatments for *P. orientalis* and this was also observed in *Q. variabilis*. Elevated [CO_2] enhanced the WUE_{ge} of *Q. variabilis* at any SWC except at 60%–80% of FC. Thirty-two saplings of *P. orientalis* had greater WUE_{ge} than did *Q. variabilis* in the same [CO_2] × SWC treatment ($p < 0.5$).

As illustrated in Fig. 5a, WUE_{cp} of *P. orientalis* in C_{600} or C_{800} increased as water stress was alleviated beyond 50%–60% of FC, as well as that in C_{400} or C_{500} while SWC exceeded 60%–70% of FC. *Q. variabilis* showed variable WUE_{cp} with SWC increased (Fig. 5b). Except for C_{400}, WUE_{cp} of *Q. variabilis* decreased abruptly at 50%–60% of FC, and then increased as SWC increased in C_{500}, C_{600}, and C_{800}. In contrast to the results of WUE_{ge}, WUE_{cp} of *Q. variabilis* was more pronounced than *P. orientalis* among all orthogonal treatments.

3.4 ^{13}C fractionation from the site of carboxylation to cytoplasm before sugars transportation

We evaluated the total ^{13}C fractionation from the site of carboxylation to the cytoplasm by gas-exchange measurements and WSCs in leaves (Table 2), which can track the path of ^{13}C fractionation in leaves. Comparing $\delta^{13}C_{WSC}$ with $\delta^{13}C_{model}$ from Eqns. (4, 7–9), the total ^{13}C fractionation of *P. orientalis* ranged from 0.0328‰ to 0.0472‰, which was less than that of *Q. variabilis* (0.0384‰ to 0.0466‰). The total fractionations of *P. orientalis* were magnified with SWC increased especially values that reached 35%–80% of FC from C_{400} to C_{800} (increased by 21.30%–42.04%). The total fractionations under C_{400} and C_{500} were amplified as SWC increased until 50%–60% of FC in *Q. variabilis*, whereas they were increased at 50%–80% of FC and decreased at 100% of FC under C_{600} and C_{800}. Elevated [CO_2] enhanced the mean total fractionation of *P. orientalis*, while fractionation of *Q. variabilis* declined sharply from C_{600} to C_{800}. Total ^{13}C fractionation, with increased SWC, in *P. orientalis* increased more rapidly than did *Q. variabilis*.

3.5 g_m imposed on the interaction of CO_2 concentration and water stress

A comparison between online leaf $\delta^{13}C_{WSC}$ and the values of gas-exchange measurements is given to estimate the g_m over all treatments in Fig. 6 (Eqns. 10–17). A significant increasing trend of g_m occurred with reduced water stress in *P. orientalis*, ranging from 0.0091–0.0690 mol·CO_2 $m^{-2}\cdot s^{-1}$ ($p< 0.5$), which reached a maximum at 100% of FC under a given [CO_2]. Increases in g_m of *Q. variabilis* with increasing SWC were not significant except those under C_{400}. With increasing [CO_2], g_m of the two species increased at different rates. With *P. orientalis* under C_{400}, g_m increased gradually and reached a maximum under C_{800} at 35%–60% of FC and 100% of FC ($p< 0.5$). However, that was maximized under C_{600} ($p< 0.5$) and reduced under C_{800} at 60%–80% of FC. The maximum increments of g_m (8.2%–58.4%) occurred at C_{800} at all SWCs in *Q. variabilis*. The g_m of *Q. variabilis* was clearly greater than that of *P. orientalis* under the same treatments.

3.6 Contribution of post-carboxylation fractionation

We evaluated the difference between Δ_i and Δ_{obs} in ^{13}C fractionation derived from mesophyll conductance. The post-photosynthetic fractionation after carboxylation can be calculated by subtracting g_m-sourced fractionation from the total ^{13}C fractionation (Table 2). The g_m-sourced fractionation provided less contribution to the total ^{13}C fractionation than that from post-carboxylation fractionation within any treatment (Table 2). The g_m-sourced fractionation in the two species illustrated different variations with SWC increased, which declined at 50%–80% of FC and increased at 100% of FC in *P. orientalis* yet, in *Q. variabilis*, it increased with water stress alleviation at 50%–80% of FC and then decreased at 100% of FC. Nevertheless, in the two species post-carboxylation fractionation in leaves and these contributions all increased as soil moisture increased. The g_m-sourced fractionation in *P. orientalis* and *Q. variabilis* reached their peaks under C_{600} and C_{800}, respectively. Post-carboxylation fractionation was magnified with [CO_2] increase in *P. orientalis*, and reached maxima under C_{600} and then were reduced under C_{800}.

3.7 Relationship between g_s, g_m and total ^{13}C fractionation

Total ^{13}C fractionation may be correlated with resistances from stomata and mesophyll cells. We performed linear regressions between g_s/g_m and total ^{13}C fractionation values for *P. orientalis* and *Q. variabilis*, respectively (Fig. 7 and 8). The total ^{13}C fractionation was correlated to the g_s ($p < 0.01$). The positive linear relationships between g_m and total ^{13}C fractionation ($p < 0.01$) indicated that the variation of [CO_2] through the chloroplast was correlated with carbon discrimination occurring after leaf photosynthesis.

4 Discussion

4.1 Photosynthetic traits

The exchange of CO_2 and water vapor via stomata can be modulated by the soil/leaf water potential (Robredo et al., 2010). Saplings of *P. orientalis* reached maximum P_n and g_s at 70%–80% of FC irrespective of [CO_2] treatments. As SWC exceeded this water threshold, elevated CO_2 caused a greater g_s reduction as was similarly reported for barley and wheat (Wall et al., 2011). The decrease of g_s responding to elevated [CO_2], could be mitigated by increased SWC. The C_i of *Q. variabilis* peaked at 60%–70% of FC and then declined as soil moisture increased (Wall et al., 2006; Wall et al., 2011). This may be because stomata tend to maintain a constant C_i or C_i/C_a when ambient [CO_2] is increased, which would determine the amount of CO_2 used directly in the chloroplast (Yu et al., 2010). This result could be explained as stomatal limitation (Farquhar and Sharkey, 1982; Xu, 1997). However, C_i of *P. orientalis* was increased considerably while SWC exceeded 70%–80% of FC, as found by Mielke et al. (2000). One possible contributing factor is plants close their stomata to reduce water loss during organic matter synthesis simultaneously decreasing the availability of CO_2 and generating respiration of organic matter (Robredo et al., 2007). Another possible explanation is that the limited root volume of potted plant experiments may be unable to absorb sufficient water to support full growth of shoots (Leakey et al., 2009; Wall et al., 2011). In the present study, increasing [CO_2] may cause nonstomatal limitation when SWC exceeds a soil moisture threshold (70%–80% of FC). The accumulation of nonstructural carbohydrates in leaf tissue may induce mesophyll-based and/or biochemical-based transient inhibition of photosynthetic capacity (Farquhar and Sharkey, 1982). Xu and Zhou (2011) developed a five-level SWC gradient to examine the effect of water on the physiology of perennial *Leymus chinensis* and demonstrated that there was a clear maximum of SWC below which the plant could adjust to changing environmental conditions. Miranda Apodaca et al. (2015) also concluded that, in suitable water conditions, elevated CO_2 levels augmented CO_2 assimilation in herbaceous plants.

The P_n of the two woody plant species increased with elevated [CO_2] similar to results from other C_3 woody plants (Kgope et al., 2010). Increasing [CO_2] alleviated severe drought and heavy irrigation, suggesting that photosynthetic inhibition produced by a lack or excess of water may be mediated by increased [CO_2] (Robredo et al., 2007; Robredo et al., 2010) and ameliorate the effects of drought stress by reducing plant transpiration (Kirkham, 2016; Kadam et al., 2014; Miranda Apodaca et al., 2015; Tausz Posch et al., 2013).

4.2 Differences between WUE_{ge} and WUE_{cp}

The increases of WUE_{ge} in *P. orientalis* and *Q. variabilis* that resulted from the combination of P_n increase and g_s decrease were followed by a reduction in T_r (Figs. 2a, 2g, 2b and 2h). This result was also demonstrated by Ainsworth and McGrath (2010). Comparing the P_n and T_r values of the two species, a lower WUE_{ge} in *Q. variabilis* was obtained due to its physiological and morphological traits, such as larger leaf area, rapid growth, and higher stomatal conductance than that of *P. orientalis*

(Adiredjo et al., 2014). Medlyn et al. (2001) reported that stomatal conductance of broadleaved species is more sensitive to elevated [CO_2] than conifer species. There is no agreement on the patterns of iWUE, at the leaf level, related to SWC (Yang et al., 2010). The WUE_{ge} of *P. orientalis* and *Q. variabilis* were enhanced with soil drying, as presented by Parker and Pallardy (1991), DeLucia and Heckathorn (1989), Reich et al. (1989), and Leakey (2009).

Bögelein et al. (2012) confirmed that WUE_{cp} was more consistent with daily mean WUE_{ge} than WUE_{phloem} (calculated by the $\delta^{13}C$ of phloem). The WUE_{cp} of the two species demonstrated similar variation to those $\delta^{13}C_{WSC}$, which differed from that of WUE_{ge}. Pons et al. (2009) noted that Δ of leaf soluble sugar is coupled with environmental dynamics over a period ranging from a few hours to 1–2 d. The WUE_{cp} of our materials could respond to [CO_2] × SWC treatments over a number of cultivated days, whereas WUE_{ge} is characterized as the instantaneous physiology change of plants to new conditions. In addition, species-specific $\delta^{13}C_{WSC}$ were observed in the same environmental treatment. Consequently, WUE_{cp} and WUE_{ge} have different degrees of variations in response to different treatments.

4.3 Influence of mesophyll conductance on the fractionation after carboxylation

CO_2 diffusion into photosynthetic sites includes two main processes. CO_2 first moves from ambient air surrounding the leaf (C_a) through stomata to the sub-stomatic cavities (C_i). From sub-stomatic cavities CO_2 then moves to the sites of carboxylation within the chloroplast stroma (C_c) of the leaf mesophyll. The latter procedure of diffusion is termed mesophyll conductance (g_m) (Flexas et al., 2008). Moreover, g_m has been identified to coordinate with environmental factors more rapidly than stomatal conductance (Galmés et al., 2007; Tazoe et al., 2011; Flexas et al., 2007). During our 7-d cultivations of SWC × [CO_2], g_m increased and WUE_{ge} decreased with increasing SWC. It has been documented that g_m can improve WUE under drought pretreatment (Han et al., 2016). However, the mechanism on which g_m responds to the fluctuation of [CO_2] is unclear. Terashima *et al.* (2006) demonstrated that CO_2 permeable aquaporin, located in the plasma membrane and inner envelope of chloroplasts, could regulate the change of g_m. In our study, g_m is species-specific to the [CO_2] gradient. The g_m of *P. orientalis* was significantly decreased by 9.08%-44.42% from C_{600} to C_{800} at 60%-80% of FC, and these are similar to the results of Flexas *et al.* (2007). A larger g_m of *Q. variabilis* under C_{800} was observed comparing with *P. orientalis*.

Furthermore, g_m contributed to the total ^{13}C fractionation that followed carboxylation while photosynthate had not been transported to the sapling twigs. The ^{13}C fractionation of CO_2 from the air surrounding the leaf to sub-stomatal cavities may be simply considered, whereas the fractionation induced by mesophyll conductance from sub-stomatic cavities to the site of carboxylation in the chloroplast cannot be neglected (Pons et al., 2009; Cano et al., 2014). In estimating the post-carboxylation fractionation, g_m-sourced fractionation must be subtracted from the total ^{13}C fractionation (the difference between $\delta^{13}C_{WSC}$ and $\delta^{13}C_{model}$), which is closely associated with g_m (Fig. 8, $p = 0.01$ or $p < 0.01$). Variations in g_m-sourced fractionation are coordinated with that of g_m with changing environmental conditions (Table 2).

4.4 Post-carboxylation fractionation generated before photosynthate moves out of leaves

Photosynthesis, a biochemical and physiological process (Badeck et al., 2005), is characterized by discrimination in ^{13}C, which leaves an isotopic signature in the photosynthetic apparatus. Farquhar *et al.* (1989) reviewed the carbon-fractionation in leaves and covered the significant aspects of photosynthetic carbon isotope discrimination. The post-carboxylation/photosynthetic fractionation associated with the metabolic pathways of non-structural carbohydrates (NSC; defined here as soluble sugars + starch) within leaves, and fractionation during translocation, storage, and remobilization prior to tree ring formation is unclear (Epron et al., 2012; Gessler et al., 2014; Rinne et al., 2016). The synthesis processes of sucrose and starch before transportation to twig fall within the domain of post-carboxylation fractionation generated in leaves. Hence, we hypothesized that ^{13}C fractionation might exist. When we completed the leaf gas-exchange measurements, leaf samples were collected immediately to determine the $\delta^{13}C_{WSC}$. Presumably, ^{13}C fractionation generated in the synthetic processes of sucrose and starch was contained within the ^{13}C fractionation from the site of carboxylation to cytoplasm before sugar transportation. Comparing $\delta^{13}C_{WSC}$ with $\delta^{13}C_{obs}$, the total ^{13}C fractionation of *P. orientalis* ranged from 0.0328‰ to 0.0472‰, which was somewhat less than that of *Q. variabilis* (from 0.0384‰ to 0.0466‰). Post-carboxylation fractionation contributed 75.30%-98.9% to total ^{13}C fractionation, determined by subtracting the fractionation of g_m from total ^{13}C fractionation. Gessler et al. (2004) reviewed the environmental components of variation in photosynthetic carbon isotope discrimination in terrestrial plants. Total ^{13}C fractionation of *P. orientalis* was enhanced by the increase of SWC, consistent with that of *Q. variabilis*, except at 100% of FC. The ^{13}C isotope signature of *P. orientalis* was depleted with elevated [CO_2]. Yet, ^{13}C-depletion was weakened in *Q. variabilis* at C_{600} and C_{800}. Linear regressions between g_s and total ^{13}C fractionation indicated that the post-carboxylation fractionation in leaves depends on the variation of g_s and that the stomata aperture was correlated with environmental change.

5 Conclusions

Through orthogonal treatments of four [CO_2]s × five SWCs, WUE_{cp} calculated by $\delta^{13}C_{WSC}$ and WUE_{ge} derived from simultaneous leaf gas-exchange, were estimated to differentiate the $\delta^{13}C$ signal variation before leaf-exported translocation of primary assimilates. The influence of g_m on ^{13}C fractionation between the sites of carboxylation and ambient environment is important. It requires consideration when testing the hypothesis that the post-carboxylation contributes to the ^{13}C fractionation from the site of carboxylation to cytoplasm before sugar transport. In response to the interactive effects of [CO_2] and SWC, WUE_{ge} of two tree species both decreased with increasing SWC, and increased with elevated [CO_2] at 35%–80% of FC. We concluded that relative soil drying, coupled with elevated [CO_2], can improve WUE_{ge} by strengthening photosynthetic capacity and reducing transpiration. WUE_{ge} of *P. orientalis* was significantly greater than that of *Q. variabilis*, while the opposite was the case for WUE_{cp}. The g_m and post-carboxylation both contributed to the total ^{13}C fractionation. This was determined by gas-exchange and carbon isotopic measurements. Rising [CO_2] and/or moistening soil generated increasing disparities between $\delta^{13}C_{WSC}$ and $\delta^{13}C_{model}$ in *P. orientalis*; nevertheless, the differences between $\delta^{13}C_{WSC}$ and $\delta^{13}C_{model}$ in *Q. variabilis* increased when [CO_2] was less than 600 ppm and/or water stress was alleviated. Total ^{13}C fractionation in leaf was linearly dependent on g_s. With respect to carbon isotope fractionation in post-carboxylation and transportation processes, we note that the ^{13}C fractionation derived from the synthesis of sucrose and starch is likely influenced by environmental changes. A clear description of the magnitude and environmental dependence of post-carboxylation fractionation is worth evaluation.

References

Adiredjo, A. L., Navaud, O., Lamaze, T., and Grieu, P.: Leaf carbon isotope discrimination as an accurate indicator of water use efficiency in sunflower genotypes subjected to five stable soil water contents, J Agron. Crop Sci., 200, 416–424, 2014.

Ainsworth, E. A. and McGrath, J. M.: Direct effects of rising atmospheric carbon dioxide and ozone on crop yields, Climate Change and Food Security, Springer, 109–130, 2010.

Badeck, F. W., Tcherkez, G., Eacute, N. S. S., Piel, C. E. M., and Ghashghaie, J.: Post-photosynthetic fractionation of stable carbon isotopes between plant organ – a widespread phenomenon, Rapid Commun. Mass S., 19, 1381–1391, 2005.

Bögelein, R., Hassdenteufel, M., Thomas, F. M., and Werner, W.: Comparison of leaf gas exchange and stable isotope signature of water-soluble compounds along canopy gradients of co-occurring Douglas-fir and European beech, Plant Cell Environ., 35, 1245–1257, 2012.

Brandes, E., Kodama, N., Whittaker, K., Weston, C., Rennenberg, H., Keitel, C., Adams, M. A., and Gessler, A.: Short-term variation in the isotopic composition of organic matter allocated from the leaves to the stem of *Pinus sylvestris*: effects of photosynthetic and postphotosynthetic carbon isotope fractionation, Global Change Biol., 12, 1922–1939, 2006.

Brooks, A. and Farquhar, G. D.: Effect of temperature on the CO_2/O_2 specificity of ribulose-1,5-bisphosphate carboxylase/oxygenase and the rate of respiration in the light, Planta, 165, 397–406, 1985.

Brugnoli E, Farquhar GD. 2000. Photosynthetic fractionation of carbon isotopes. In: Leegood RC, Sharkey TD, von Caemmerer S. eds. Photosynthesis: physiology and metabolism. Advances in photosynthesis. Dordrecht, The Netherlands: Kluwer Academic Publishers, 399–434.

Cano, F. J., López, R., and Warren, C. R.: Implications of the mesophyll conductance to CO_2 for photosynthesis and water-use efficiency during long-term water stress and recovery in two contrasting Eucalyptus species, Plant Cell Environ., 37, 2470–2490, 2014.

Cernusak, L. A., Ubierna, N., Winter, K., Holtum, J. A. M., Marshall, J. D., and Farquhar, G. D.: Environmental and physiological determinants of carbon isotope discrimination in terrestrial plants, New Phytologist, 200, 950–965, 2013.

DeLucia, E. H. and Heckathorn, S. A.: The effect of soil drought on water-use efficiency in a contrasting Great Basin desert and Sierran montane species, Plant Cell Environ., 12, 935–940, 1989.

Epron, D., Nouvellon, Y., and Ryan, M. G.: Introduction to the invited issue on carbon allocation of trees and forests, Tree physiol., 32, 639–643, 2012.

Evans, J. R., Kaldenhoff, R., Genty, B., and Terashima, I.: Resistances along the CO_2 diffusion pathway inside leaves, J. Exp. Bot., 60, 2235–2248, 2009.

Evans, J. R., Sharkey, T. D., Berry, J. A., and Farquhar, G. D.: Carbon isotope discrimination measured concurrently with gas-exchange to investigate CO_2 diffusion in leaves of higher-plants, Funct. Plant Biol., 13, 281–292, 1986.

Evans, J. R. and von Caemmerer, S.: Temperature response of carbon isotope discrimination and mesophyll conductance in tobacco, Plant Cell Environ., 36, 745–756, 2013.

Farquhar, G. D., Ehleringer, J. R., and Hubick, K. T.: Carbon isotope discrimination and photosynthesis, Ann. Rev. Plant Physiol., 40, 503–537, 1989.

Farquhar, G. D., O'Leary, M. H., and Berry, J. A.: On the relationship between carbon isotope discrimination and the intercellular carbon dioxide concentration in leaves, Funct. Plant Biol., 9, 121–137, 1982.

Farquhar, G. D. and Sharkey, T. D.: Stomatal conductance and photosynthesis, Ann. Rev. Plant

Physiol., 33, 317–345, 1982.
Flexas, J., Barbour, M. M., Brendel, O., Cabrera, H. M., Carriquí, M., Díaz-Espejo, A., Douthe, C., Dreyer, E., Ferrio, J. P., Gago, J., Gallé, A., Galmés, J., Kodama, N., Medrano, H., Niinemets, Ü., Peguero-Pina, J. J., Pou, A., Ribas-Carbó, M., Tomás, M., Tosens, T., and Warren, C. R.: Mesophyll diffusion conductance to CO_2: An unappreciated central player in photosynthesis, Plant Science, 193–194, 70–84, 2012.
Flexas, J., Carriquí, M., Coopman, R. E., Gago, J., Galmés, J., Martorell, S., Morales, F., and Diaz-Espejo, A.: Stomatal and mesophyll conductances to CO_2 in different plant groups: Underrated factors for predicting leaf photosynthesis responses to climate change? Plant Science, 226, 41–48, 2014.
Flexas, J., Diaz-Espejo, A., Galmés, J., Kaldenhoff, R., Medano, H., and Ribas-Carbo, M.: Rapid variations of mesophyll conductance in response to changes in CO_2 concentration around leaves, Plant Cell Environ., 30, 1284–1298, 2007.
Flexas, J., Ribas-Carbó, M., Diaz-Espejo, A., Galmés, J., and Medrano, H.: Mesophyll conductance to CO_2: current knowledge and future prospects, Plant Cell Environ., 31, 602–621, 2008.
Flexas, J., Ribas-Carbó, M., Hanson, D.T., Bota, J., Otto, B., Cifre, J., McDowell, N., Medrano, H., and Kaldenhoff, R.: Tobacco aquaporin NtAQP1 is involved in mesophyll conductance to CO_2 *in vivo*, Plant J., 48, 427–439, 2006.
Galmés, J., Medrano, H., and Flexas, J.: Photosynthetic limitations in response to water stress and recovery in Mediterranean plants with different growth forms, New Phytol., 175, 81–93. 2007.
Gessler, A., Brandes, E., Buchmann, N., Helle, G., Rennenberg, H., and Barnard, R. L.: Tracing carbon and oxygen isotope signals from newly assimilated sugars in the leaves to the tree-ring archive, Plant Cell Environ., 32, 780–795, 2009.
Gessler, A., Ferrio, J. P., Hommel, R., Treydte, K., Werner, R. A., and Monson, R. K.: Stable isotopes in tree rings: towards a mechanistic understanding of isotope fractionation and mixing processes from the leaves to the wood, Tree Physiol., 34, 796–818, 2014.
Gessler, A., Rennenberg, H., and Keitel, C.: Stable isotope composition of organic compounds transported in the phloem of European beech-evaluation of different methods of phloem sap collection and assessment of gradients in carbon isotope composition during leaf-to-stem transport, Plant Biology, 6, 721–729, 2004.
Gessler, A., Tcherkez, G., Peuke, A. D., Ghashghaie, J., and Farquhar, G. D.: Experimental evidence for diel variations of the carbon isotope composition in leaf, stem and phloem sap organic matter in *Ricinus communis*, Plant Cell Environ., 31, 941–953, 2008.
Gillon, J. S., Griffiths, H.: The influence of (photo)respiration on carbon isotope discrimination in plants. Plant Cell Environ., 20, 1217–1230, 1997.
Gleixner, G. and Schmidt, H.: Carbon isotope effects on the fructose-1, 6-bisphosphate aldolase reaction, origin for non-statistical ^{13}C distributions in carbohydrates, J. Biol. Chem., 272, 5382–5387, 1997.
Guy, R. D., Fogel, M. L., and Berry, J. A.: Photosynthetic fractionation of the stable isotopes of oxygen and carbon, Plant Physiol., 101, 37–47, 1993.
Han, J. M., Meng, H. F., Wang, S. Y., Jiang, C. D., Liu, F., Zhang, W. F., and Zhang, Y. L.: Variability of mesophyll conductance and its relationship with water use efficiency in cotton leaves under drought pretreatment, J. Plant Physiol., 194, 61–71, 2016.
Hommel, R., Siegwolf, R., Saurer, M., Farquhar, G. D., Kayler, Z., Ferrio, J. P., and Gessler, A.:

Drought response of mesophyll conductance in forest understory species-impacts on water-use efficiency and interactions with leaf water movement, Physiol. Plantarum, 152, 98–114, 2014.

Igamberdiev, A. U., Mikkelsen, T. N., Ambus, P., Bauwe, H., and Lea, P. J.: Photorespiration contributes to stomatal regulation and carbon isotope fractionation: a study with barley, potato and Arabidopsis plants deficient in glycine decarboxylase, Photosynth. Res., 81, 139–152, 2004.

IPCC: Summary for policymakers, in: Climate Change 2014, Mitigation of Climate Change, contribution of Working Group III to the Fifth Assessment Report of the Intergovernmental Panel on Climate Change, edited by: Edenhofer, O., Pichs-Madruga, R., Sokona, Y., Farahani, E., Kadner, S., Seyboth, K., Adler, A., Baum, I., Brunner, S., Eickemeier, P., Kriemann, B., Savolainen, J., Schlomer, S., von Stechow, C., Zwickel, T., and Minx, J. C., Cambridge University Press, Cambridge, UK and New York, NY, USA, 1–30, 2014.

Jäggi, M., Saurer, M., Fuhrer, J., and Siegwolf, R.: The relationship between the stable carbon isotope composition of needle bulk material, starch, and tree rings in *Picea abies*, Oecologia, 131, 325–332, 2002.

Kadam, N. N., Xiao, G., Melgar, R. J., Bahuguna, R. N., Quinones, C., Tamilselvan, A., Prasad, P. V. V., and Jagadish, K. S. V.: Chapter three-agronomic and physiological responses to high temperature, drought, and elevated CO_2 interactions in cereals, Adv. Agron., 127, 111–156, 2014.

Kgope, B. S., Bond, W. J., and Midgley, G. F.: Growth responses of African savanna trees implicate atmospheric [CO_2] as a driver of past and current changes in savanna tree cover, Austral Ecol., 35, 451–463, 2010.

Kirkham, M. B.: Elevated carbon dioxide: impacts on soil and plant water relations, CRC Press, London, New York, 2016.

Kodama, N., Barnard, R. L., Salmon, Y., Weston, C., Ferrio, J. P., Holst, J., Werner, R. A., Saurer, M., Rennenberg, H., and Buchmann, N.: Temporal dynamics of the carbon isotope composition in a *Pinus sylvestris* stand: from newly assimilated organic carbon to respired carbon dioxide, Oecologia, 156, 737–750, 2008.

Lanigan, G. J., Betson, N., Griffiths, H., and Seibt, U.: Carbon isotope fractionation during photorespiration and carboxylation in Senecio, Plant Physiol., 148, 2013–2020, 2008.

Le Roux, X., Bariac, T., Sinoquet H., Genty, B., Piel, C., Mariotti, A., Girardin, C., and Richard, P.: Spatial distribution of leaf water-use efficiency and carbon isotope discrimination within an isolated tree crown, Plant Cell Environ., 24, 1021–1032, 2001.

Leakey, A. D.: Rising atmospheric carbon dioxide concentration and the future of C4 crops for food and fuel, Proceedings of the Royal Society of London B: Biological Sciences, 276, 1517–2008, 2009.

Leakey, A. D., Ainsworth, E. A., Bernacchi, C. J., Rogers, A., Long, S. P., and Ort, D. R.: Elevated CO_2 effects on plant carbon, nitrogen, and water relations: six important lessons from FACE, J. Exp. Bot., 60, 2859–2876, 2009.

Lobell, D. B., Roberts, M. J., Schlenker, W., Braun, N., Little, B. B., Rejesus, R. M., and Hammer, G. L.: Greater sensitivity to drought accompanies maize yield increase in the US Midwest, Science, 344, 516–519, 2014.

Medlyn, B. E., Barton, C. V. M., Broadmeadow, M. S. J., Ceulemans, R., Angelis, P. D., Forstreuter, M., Freeman, M., Jackson, S. B., Kellomäki, S., and Laitat, E.: Stomatal conductance of forest species after long-term exposure to elevated CO_2 concentration: a synthesis, New Phytol., 149, 247–264, 2001.

Mielke, M. S., Oliva, M. A., de Barros, N. F., Penchel, R. M., Martinez, C. A., Da Fonseca, S., and de Almeida, A. C.: Leaf gas exchange in a clonal eucalypt plantation as related to soil moisture, leaf water potential and microclimate variables, Trees, 14, 263–270, 2000.

Miranda Apodaca, J., Pérez López, U., Lacuesta, M., Mena Petite, A., and Muñoz Rueda, A.: The type of competition modulates the ecophysiological response of grassland species to elevated CO_2 and drought, Plant Biolog, 17, 298–310, 2015.

Parker, W. C. and Pallardy, S. G.: Gas exchange during a soil drying cycle in seedlings of four black walnut (*Juglans nigra* l.) Families, Tree physiol., 9, 339–348, 1991.

Pons, T. L., Flexas, J., von Caemmerer, S., Evans, J. R., Genty, B., Ribas-Carbo, M., and Brugnoli, E.: Estimating mesophyll conductance to CO_2: methodology, potential errors, and recommendations, J. Exp. Bot., 8, 1–18, 2009.

Reich, P. B., Walters, M. B., and Tabone, T. J.: Response of *Ulmus americana* seedlings to varying nitrogen and water status. 2 Water and nitrogen use efficiency in photosynthesis, Tree Physiol., 5, 173–184, 1989.

Rinne, K. T., Saurer, M., Kirdyanov, A. V., Bryukhanova, M. V., Prokushkin, A. S., Churakova Sidorova, O. V., and Siegwolf, R. T.: Examining the response of larch needle carbohydrates to climate using compound-specific $\delta^{13}C$ and concentration analyses, EGU General Assembly Conference, 1814949R, 2016.

Robredo, A., Pérez-López, U., de la Maza, H. S., González-Moro, B., Lacuesta, M., Mena-Petit,e A., and Muñoz-Rueda, A.: Elevated CO_2 alleviates the impact of drought on barley improving water status by lowering stomatal conductance and delaying its effects on photosynthesis, Environ. Exp. Bot., 59, 252–263, 2007.

Robredo, A., Pérez-López, U., Lacuesta, M., Mena-Petite, A., and Muñoz-Rueda, A.: Influence of water stress on photosynthetic characteristics in barley plants under ambient and elevated CO_2 concentrations, Biologia. Plantarum, 54, 285–292, 2010.

Rossmann, A., Butzenlechner, M., and Schmidt, H.: Evidence for a nonstatistical carbon isotope distribution in natural glucose, Plant Physiol., 96, 609–614, 1991.

Streit, K., Rinne, K. T., Hagedorn, F., Dawes, M. A., Saurer, M., Hoch, G., Werner, R. A., Buchmann, N., and Siegwolf, R. T. W.: Tracing fresh assimilates through *Larix decidua* exposed to elevated CO_2 and soil warming at the alpine treeline using compound-specific stable isotope analysis, New Phytol., 197, 838–849, 2013.

Tausz Posch, S., Norton, R. M., Seneweera, S., Fitzgerald, G. J., and Tausz, M.: Will intra-specific differences in transpiration efficiency in wheat be maintained in a high CO_2 world? A FACE study, Physiol. Plantarum, 148, 232–245, 2013.

Tazoe, Y., von Caemmerer, S., Estavillo, G. M., and Evans, J. R.: Using tunable diode laser spectroscopy to measure carbon isotope discrimination and mesophyll conductance to CO_2 diffusion dynamically at different CO_2 concentrations, Plant Cell Environ., 34, 580–591, 2011.

Terashima, I., Hanba, Y.T., Tazoe, Y., Vyas, P., and Yano, S.: Irradiance and phenotype: comparative eco-development of sun and shade leaves in relation to photosynthetic CO_2 diffusion, J. Exp. Bot., 57, 343–354, 2006.

Théroux-Rancourt, G., Éthier, G., and Pepin, S.: Threshold response of mesophyll CO_2 conductance to leaf hydraulics in highly transpiring hybrid poplar clones exposed to soil drying, J. Exp. Bot., 65, 741-753, 2014.

Von Caemmerer, S. V. and Farquhar, G. D.: Some relationships between the biochemistry of photosynthesis and the gas exchange of leaves, Planta, 153, 376–387, 1981.

Wall, G. W., Garcia, R. L., Kimball, B. A., Hunsaker, D. J., Pinter, P. J., Long, S. P., Osborne, C. P., Hendrix, D. L., Wechsung, F., and Wechsung, G.: Interactive effects of elevated carbon dioxide and drought on wheat, Agron. J., 98, 354–381, 2006.

Wall, G. W., Garcia, R. L., Wechsung, F., and Kimball, B. A.: Elevated atmospheric CO_2 and drought effects on leaf gas exchange properties of barley, Agr. Ecosyst. Environ., 144, 390–404, 2011.

Warren, C. R. and Adams, M. A.: Internal conductance does not scale with photosynthetic capacity: implications for carbon isotope discrimination and the economics of water and nitrogen use in photosynthesis, Plant Cell Environ., 29, 192–201, 2006.

Xu, D. Q.: Some problems in stomatal limitation analysis of photosynthesis, Plant Physiol. J., 33, 241–244, 1997.

Xu, Z. and Zhou, G.: Responses of photosynthetic capacity to soil moisture gradient in perennial rhizome grass and perennial bunchgrass, BMC Plant Boil., 11, 21, 2011.

Yang, B., Pallardy, S. G., Meyers, T. P., GU, L. H., Hanson, P. J., Wullschleger, S. D., Heuer, M., Hosman, K. P., Riggs, J. S., and Sluss D. W.: Environmental controls on water use efficiency during severe drought in an Ozark Forest in Missouri, USA, Global Change Biol., 16, 2252–2271, 2010.

Yu, G., Wang, Q., and Mi, N.: Ecophysiology of plant photosynthesis, transpiration, and water use, Science Press, Beijing, China, 2010.

Author contributions

N. Zhao and Y. He collected field samples, and performed experiments. N. Zhao performed data analysis and wrote the paper. P. Meng commented on the theory and study design. X. Yu revised and edited the manuscript.

Acknowledgements. Financial support for this project was provided by the National Natural Science Foundation of China (grant No. 41430747) and the Beijing Municipal Education Commission (CEFF-PXM2017_014207_000043). We thank Beibei Zhou and Yuanhai Lou for collection of materials and management of saplings. We are grateful to anonymous reviewers for constructive suggestions regarding this manuscript. Due to space limitations we cited selected references involving this study topic and apologize for authors whose work was not cited.

Figure

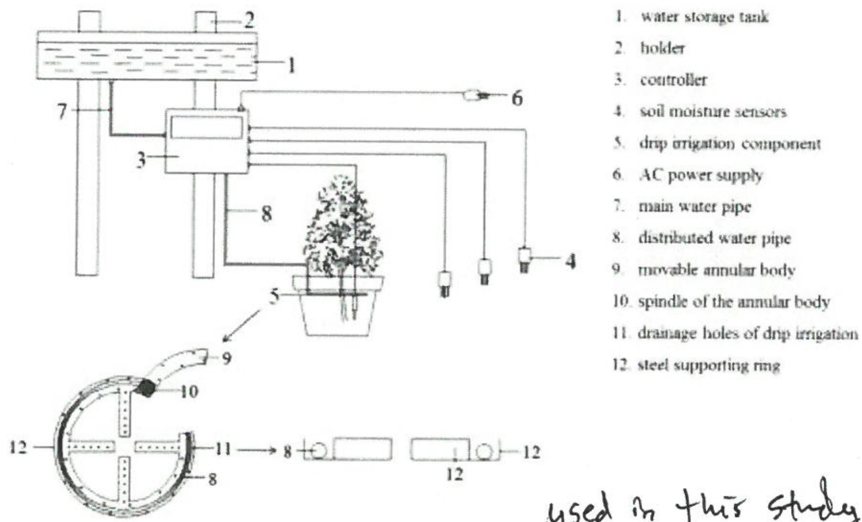

Figure 1. Diagram of the automatic drip irrigation device used in this study; Numbers indicate the individual parts of the ~~automatic drip~~ irrigation device (No. 1–12). The lower-left corner of this figure presents the detailed schematic for the drip irrigation components (No. 8–12).

the Figure needs improvement; Considerably blurry.

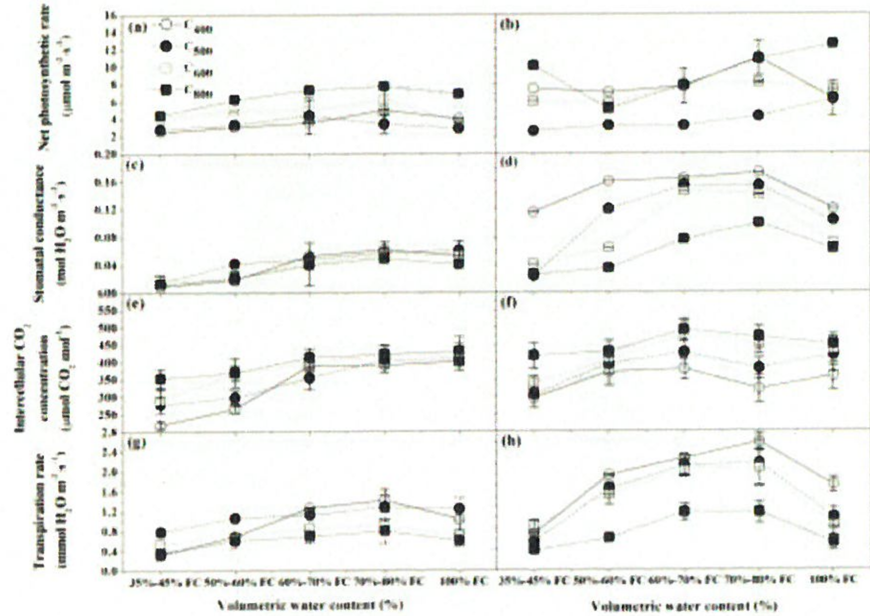

Figure 2. Net photosynthetic rates (P_n, μmol m^{-2} s^{-1}, a and b), stomatal conductance (g_s, mol H_2O m^{-2} s^{-1}, c and d), intercellular CO_2 concentration (C_i, μmol CO_2 mol^{-1}, e and f), and transpiration rates (T_r, mmol H_2O m^{-2} s^{-1}, g and h) of *P. orientalis* and *Q. variabilis* for four CO_2 concentrations × five soil volumetric water contents. Means ± SDs, n= 32.

Figures are of poor quality – please remedy.

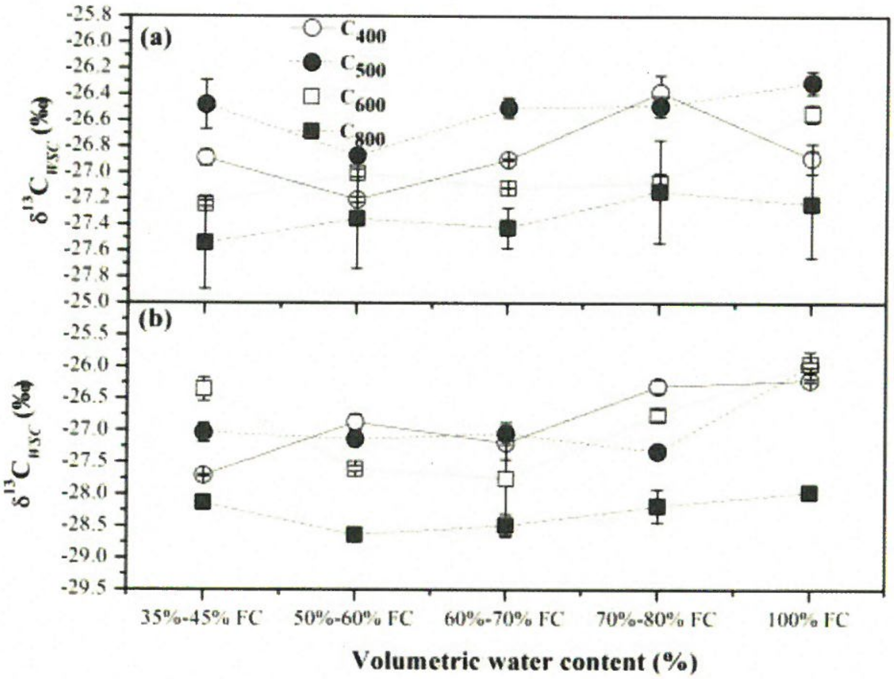

Figure 3. Carbon isotope composition of water-soluble compounds ($\delta^{13}C_{WSC}$) extracted from leaves of *P. orientalis* (a) and *Q. variabilis* (b) for four CO_2 concentrations × five soil volumetric water contents; treatments. Means ± SDs, n= 32.

Fix – improve visual quality!

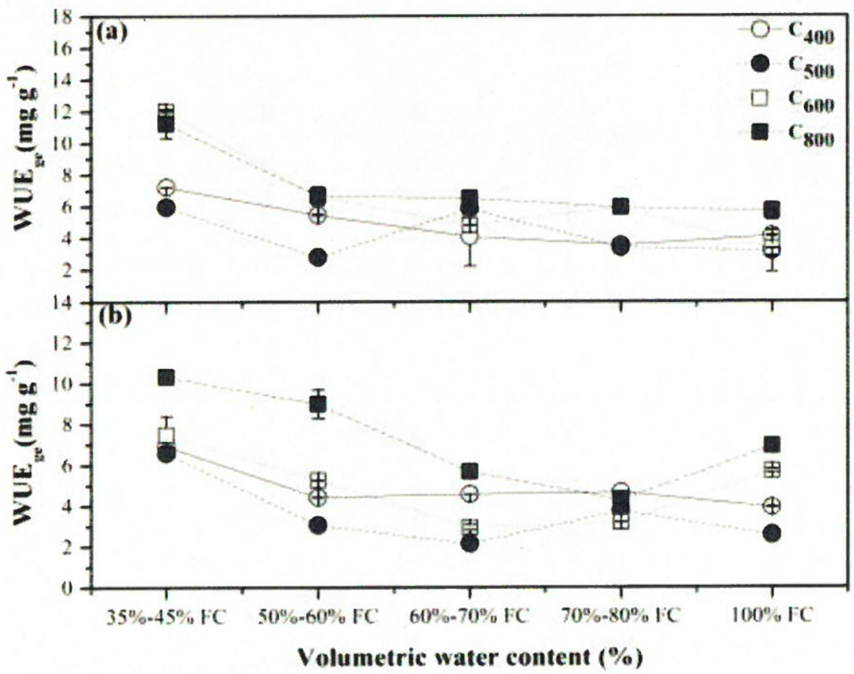

Figure 4. Instantaneous water use efficiency through gas exchange measurements (WUE_{ge}) for leaves of *P. orientalis* (a) and *Q. variabilis* (b) for four CO_2 concentrations × five soil volumetric water contents. Means ± SDs, n= 32.

from

treatments

Fix – poor quality

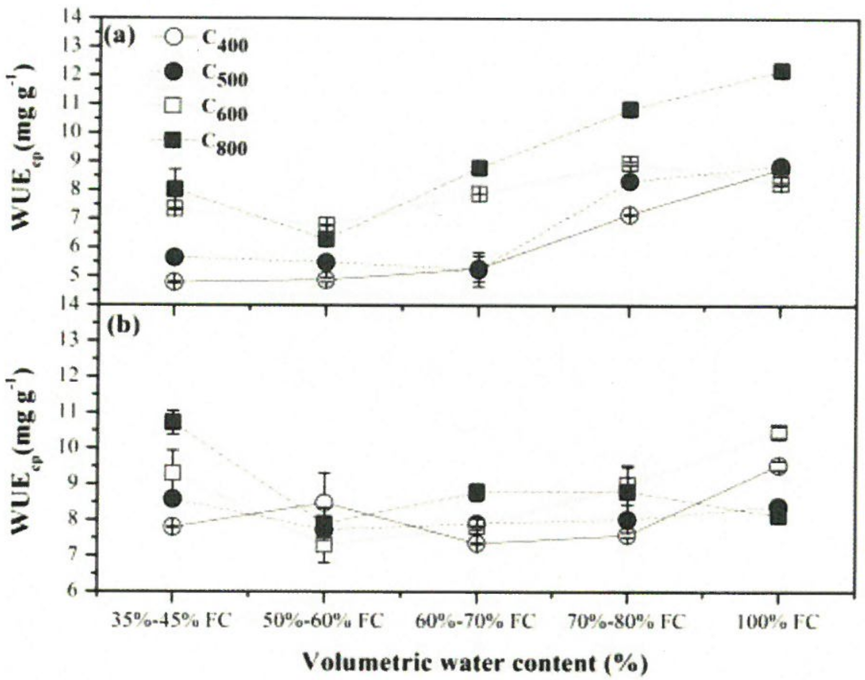

Figure 5. Instantaneous water use efficiency estimated by $\delta^{13}C$ of water-soluble compounds (WUE_{cp}) from leaves of *P. orientalis* (a) and *Q. variabilis* (b) for four CO_2 concentrations × five soil volumetric water contents. Means ± SDs, n= 32.

Fix

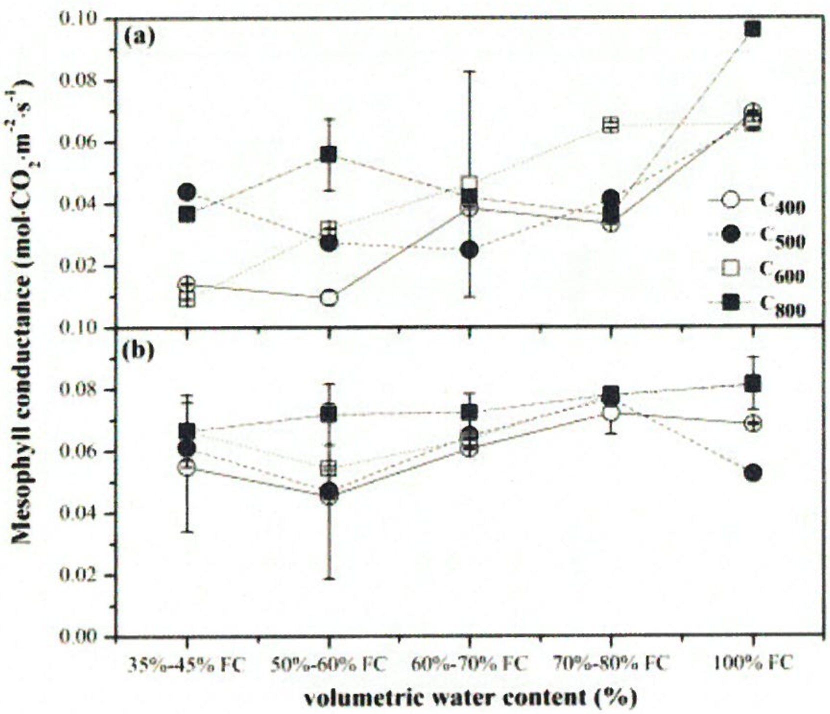

Figure 6. Mesophyll conductance of *P. orientalis* (a) and *Q. variabilis* (b) for four CO_2 concentrations × five soil volumetric water contents. Means ± SDs, n= 32.

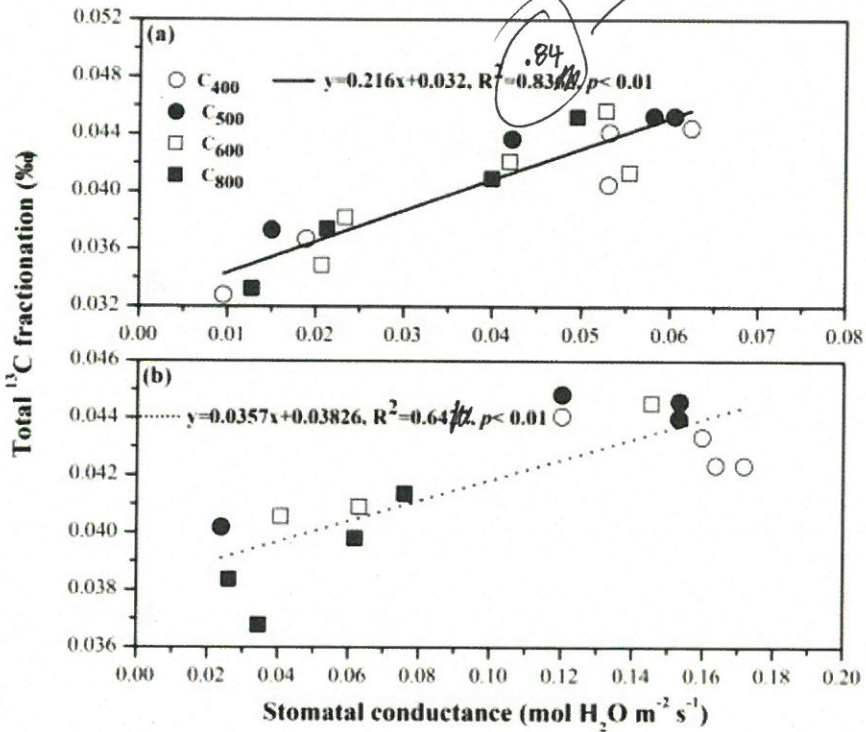

Figure 7. Regression between stomatal conductance and total ^{13}C fractionation of *P. orientalis* (a) and *Q. variabilis* (b) for four CO_2 concentrations × five soil volumetric water contents ($p= 0.01$, n= 32).

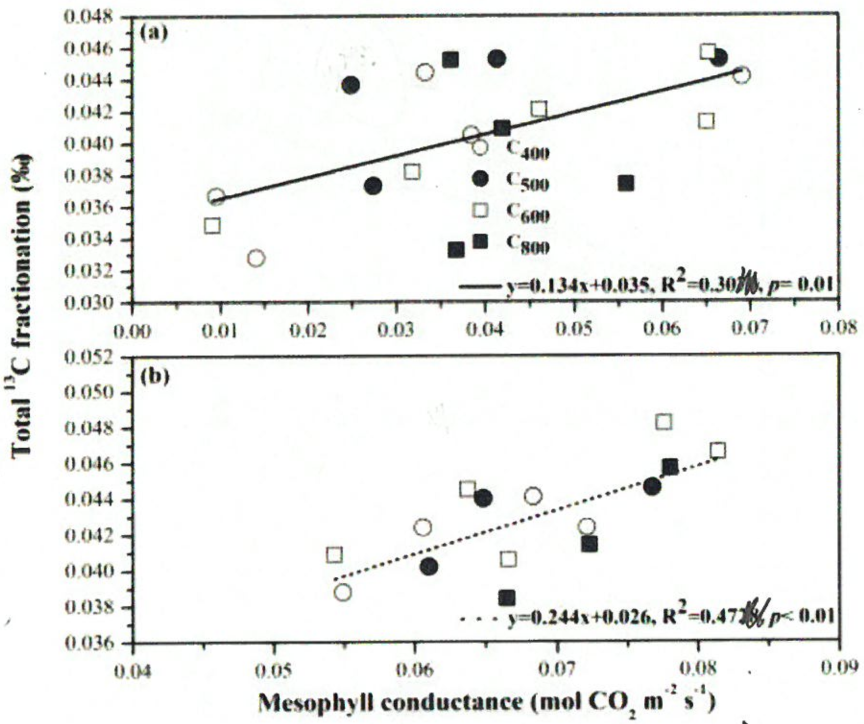

Figure 8. Regression between mesophyll conductance and total ^{13}C fractionation of *P. orientalis* (a) and *Q. variabilis* (b) for four CO_2 concentrations × five soil volumetric water contents (p= 0.01, n= 32).

treatments

Fix graph.

Table

Table 1. Orthogonal treatments of *P. orientalis* and *Q. variabilis* ~~for four CO_2 concentrations × five soil volumetric water contents~~.

P. orientalis	Repeats (cultivated period)	B_1	B_2	B_3	B_4	B_5
A_1	R_1:June 2–9	$A_1B_1R_1$	$A_1B_2R_1$	$A_1B_3R_1$	$A_1B_4R_1$	$A_1B_5R_1$
	R_2:June 12–19	$A_1B_1R_2$	$A_1B_2R_2$	$A_1B_3R_2$	$A_1B_4R_2$	$A_1B_5R_2$
A_2	R_1:July 11–18	$A_2B_1R_1$	$A_2B_2R_1$	$A_2B_3R_1$	$A_2B_4R_1$	$A_2B_5R_1$
	R_2:July 22–29	$A_2B_1R_2$	$A_2B_2R_2$	$A_2B_3R_2$	$A_2B_4R_2$	$A_2B_5R_2$
A_3	R_1:June 2–9	$A_3B_1R_1$	$A_3B_2R_1$	$A_3B_3R_1$	$A_3B_4R_1$	$A_3B_5R_1$
	R_2:June 12–19	A_3B_1R	$A_3B_2R_2$	$A_3B_3R_2$	$A_3B_4R_2$	$A_3B_5R_2$
A_4	R_1:July 11–18	$A_4B_1R_1$	$A_4B_2R_1$	$A_4B_3R_1$	$A_4B_4R_1$	$A_4B_5R_1$
	R_2:July 22–29	$A_4B_1R_2$	$A_4B_2R_2$	$A_4B_3R_2$	$A_4B_4R_2$	$A_4B_5R_2$
Q. variabilis	Repeats (cultivated period)	B_1	B_2	B_3	B_4	B_5
A_1	P_1:June 21–28	$A_1B_1P_1$	$A_1B_2P_1$	$A_1B_3P_1$	$A_1B_4P_1$	$A_1B_5R_1$
	P_2:July 2–9	$A_1B_1P_2$	$A_1B_2P_2$	$A_1B_3P_2$	$A_1B_4P_2$	$A_1B_5R_2$
A_2	P_1:August 4–11	$A_2B_1P_1$	$A_2B_2P_1$	$A_2B_3P_1$	$A_2B_4P_1$	$A_2B_5R_1$
	P_2:August 15–22	$A_2B_1P_2$	$A_2B_2P_2$	$A_2B_3P_2$	$A_2B_4P_2$	$A_2B_5R_2$
A_3	P_1:June 21–28	$A_3B_1P_1$	$A_3B_2P_1$	$A_3B_3P_1$	$A_3B_4P_1$	$A_3B_5R_1$
	P_2:July 2–9	$A_3B_1P_2$	$A_3B_2P_2$	$A_3B_3P_2$	$A_3B_4P_2$	$A_3B_5R_2$
A_4	P_1:August 4–11	$A_4B_1P_1$	$A_4B_2P_1$	$A_4B_3P_1$	$A_4B_4P_1$	$A_4B_5R_1$
	P_2:August 15–22	$A_4B_1P_2$	$A_4B_2P_2$	$A_4B_3P_2$	$A_4B_4P_2$	$A_4B_5R_2$

Table 2. Carbon-13 isotope fractionation of *P. orientalis* and *Q. variabilis* for four CO_2 concentrations × five soil volumetric water contents

Species	SWC (of FC)		CO_2 concentration (ppm) 400	500	600	800		400	500	600	800		400	500	600	800
P. orientalis	35%–45%	Total ^{13}C fractionation (‰)	0.0328	0.0373	0.0349	0.0332	Mesophyll conductance ^{13}C fractionation (‰)	0.0081	0.0030	0.0034	0.0072	Post-photosynthesis ^{13}C fractionation (‰)	0.0247	0.0343	0.0315	0.0260
	50%–60%		0.0367	0.0437	0.0382	0.0374		0.0018	0.0058	0.0094	0.0004		0.0349	0.0379	0.0288	0.0370
	60%–70%		0.0405	0.0366	0.0421	0.0409		0.0018	0.0050	0.0026	0.0007		0.0387	0.0316	0.0395	0.0402
	70%–80%		0.0444	0.0453	0.0413	0.0452		0.0044	0.0052	0.0103	0.0013		0.0400	0.0401	0.0310	0.0439
	100%		0.0441	0.0453	0.0456	0.0472		0.0057	0.0040	0.0025	0.0039		0.0384	0.0413	0.0431	0.0433
Q. variabilis	35%–45%		0.0388	0.0402	0.0406	0.0384		0.0007	0.0025	0.0006	0.0091		0.0381	0.0377	0.0400	0.0293
	50%–60%		0.0433	0.0448	0.0409	0.0368		0.0061	0.0084	0.0023	0.0018		0.0372	0.0364	0.0386	0.0350
	60%–70%		0.0424	0.0440	0.0445	0.0414		0.0066	0.0086	0.0078	0.0041		0.0358	0.0354	0.0367	0.0373
	70%–80%		0.0424	0.0446	0.0482	0.0457		0.0034	0.0016	0.0074	0.0028		0.0390	0.0430	0.0408	0.0429
	100%		0.0441	0.0466	0.0466	0.0398		0.0027	0.0076	0.0022	0.0125		0.0414	0.0390	0.0444	0.0273